Journal of Catalysis **189,** 297–313 (2000)
doi:10.1006/jcat.1999.2678, available online at http://www.idealibrary.com on IDEAL®

Propylene Oxidation over Poly(azomethines) Doped with Heteropolyacids

Wincenty Turek,* Edyta-Stochmal-Pomarzańska,†,[1] Adam Proń,‡ and Jerzy Haber§

*Institute of Physical Chemistry and Technology of Polymers, Silesian Technical University, Strzody 9, 44 100 Gliwice, Poland; †Department of Materials Sciences and Ceramics, Academy of Mining and Metallurgy, Al.Mickiewicza 30, 30 059 Kraków, Poland; ‡Department of Chemistry, Warsaw University of Technology, Noakowskiego 3, 00 664 Warszawa, Poland, and CEA Grenoble DRFMC/SI3M/PMS, 17 rue des Martyrs, 38 054 Grenoble, France; and §Institute of Catalysis and Surface Chemistry, Polish Academy of Sciences, Niezapominajek, 30 239 Kraków, Poland

Received April 22, 1999; revised September 7, 1999; accepted September 9, 1999

Kinetic studies of propylene oxidation and isopropanol conversion were undertaken using new catalytic systems, namely, conjugated polymer-supported heteropolyacid catalysts. Unsubstituted and dimethoxy-substituted aromatic poly(azomethines) (PPI and PMOPI) were used as matrices to which selected heteropolyanions (HPAs) were introduced via acid–base-type doping which consists of protonation of imine nitrogen. PPI was synthesized via polycondensation of 1,4-phenylenediamine with terephthaldehyde, whereas PMOPI was prepared via the reaction of 1,4-phenylenediamine with 2,5-dimethoxyterephthaldehyde. Protonation of PPI and PMOPI with heteropolyacids—$H_3PW_{12}O_{40}$ and $H_3PMo_{12}O_{40}$—was carried out in the acetonitrile solutions. The protonation level was controlled by changing the starting molar ratio of HPA : polymer in the reaction medium. Both poly(azomethines) in their base forms and protonated poly(azomethines) were characterized using X-ray diffraction and various spectroscopic methods (FTIR, Raman, XPS). Thermal stability and BET surface area were also studied. X-Ray diffraction patterns show that HPA introduced into the polymer matrices is molecularly dispersed and does not form a separate phase. FTIR studies prove that the structural identity of individual heteropolyanions is preserved on introduction into the polymer matrices. However, Raman studies prove that protonation leads to changes in polymer chain conformation. In the oxidation of propylene the PPI(HPA)$_y$ and PMOPI(HPA)$_y$ catalysts give hexadiene as the main reaction product. Introduction of HPA into the polymer matrices changes the selectivity of the acid since the reaction carried out in the presence of crystalline $H_3PMo_{12}O_{40}$ results in acrolein as the main product. For all catalysts studied, only products of nondestructive oxidation can be detected (hexadiene, acrolein, propionaldehyde, acetone, benzene).

Key Words: **poly(azomethines); heteropolyanions; nondestructive oxidation.**

INTRODUCTION

Conjugated polymers have been extensively studied for the last 20 years mainly due to their unusual electronic, electrochemical, and electrooptic properties (1, 2). However, these systems may also exhibit extremely interesting catalytic properties provided that they are doped with catalytically active species, for example, heteropolyanions. The first successful incorporation of heteropolyanions into polyconjugated matrices was achieved by electropolymerization of suitable heterocyclic monomers in the presence of heteropolyacids (3, 4). In this procedure heteropolyanions are introduced into the polymer matrix *in situ* during the electropolymerization process.

We have used a different approach in the preparation of conjugated polymer-supported heteropolyacid catalysts. First we prepared a neutral matrix of a given conjugated polymer to which heteropolyanions were introduced by chemical or electrochemical doping. For example, by oxidative doping of neutral polyacetylene with $H_3PMo_{12}O_{40}$ we obtained a new catalytic system extremely active in alcohol conversion reactions (5).

We have introduced heteropolyanions into conjugated polymers such as polyaniline and selected poly(azomethines), which contain basic sites, via an acid–base-type of doping that consists of protonation of imine nitrogen with heteropolyacids. Catalysts prepared by this method were also tested in alcohol conversion (6, 7).

Aromatic poly(azomethines) of the general formula

$$(=HCArCH=NArN=)_n$$

are especially well suited for use in heterogeneous catalysis because they exhibit excellent, for a polymeric system, thermal stability in both the neutral (undoped) and heteropolyacid-doped forms (7). Taking into account this enhanced thermal stability we have decided to test poly(azomethine)-supported heteropolyacid catalysts in another technologically important reaction, namely, olefin oxidation.

The process of olefin oxidation may take place on metal or metal oxide catalysts. In the majority of cases the reaction is carried out using solid solutions of oxides, mixtures of oxides, or mixtures of oxysalts as catalysts (8–16).

[1] To whom correspondence should be addressed. Fax: (48–12)633–71–61. E-mail: stochmal@uci.agh.edu.pl.

0021-9517/00 $35.00

In catalytic oxidation of hydrocarbons on oxide catalysts two different intermediate complexes initiate two different routes of the reaction (17–21). When oxygen is activated ionic radical oxygen species O^- and O_2^- are formed; these are the main oxidizing species in the total oxidation of simple molecules such as H_2, CO, and CH_4. They may be considered electrophilic reagents, which in reactions with olefins attack the molecule in the region of highest electron density. Such electrophilic addition of O_2^- or O^- results in the formation of peroxy or epoxy complexes, respectively, which under the conditions of heterogeneous catalytic oxidation are intermediates of the degradation of the carbon skeleton and total oxidation. These reactions may be classified as electrophilic oxidation (22–24). The second route of heterogeneous oxidation starts with activation of the hydrocarbon molecule by abstraction of hydrogen from a given carbon atom, which becomes prone to nucleophilic addition of the oxide ion O^{2-}. It should be emphasized that the latter has no oxidizing properties, but is a nucleophilic reactant. The consecutive steps of hydrogen abstraction and oxygen addition may then be repeated to obtain selectively more oxygenated molecules. These reactions are classified as nucleophilic oxidation (22–24). The role of oxidizing agents in these steps of the reaction sequence is played by cations of the catalyst lattice. After the nucleophilic addition of the lattice oxygen ion the oxygenated product is desorbed, leaving a vacancy at the catalyst surface.

For a long time heteropolycompounds were studied as selective oxidation catalysts (22–24). Heteropolyacids with Keggin structure are particularly attractive for mechanistic studies since they present a well-characterized surface and the versatility of their composition allows one to control easily the acidic and redox properties. They provide nucleophilic oxygen, the reactivity of which may be controlled, and do not generate electrophilic oxygen.

As already mentioned poly(azomethines) are not inert catalytic supports. The introduction of heteropolyacids to these polymers occurs via the protonation reaction of imine nitrogens. As a result catalytically active centers are molecularly dispersed and strongly chemically bonded to the polymer (7). The surface of the active phase of poly(azomethine)-supported catalysts exhibits properties significantly different from those of crystalline catalysts. As a consequence of molecular dispersion and of the lack of lattice defects characteristic of crystalline solids no electrophilic forms of chemisorbed oxygen can exist on the surface. In the catalytic process only O^{2-} (i.e., nucleophilic form of oxygen) originating from individual Keggin units can participate.

Thus heteropolyacid-doped poly(azomethines) are interesting not only as new catalysts but also as suitable catalytic systems for better elucidation of the mechanism of olefin oxidation. In addition to physicochemical characterization of these new catalysts, one of the goals of this research was to determine how the reduction in the number of active forms of oxygen influences the selectivity of the oxidation process.

EXPERIMENTAL

Two types of polymer matrices were synthesized: the simplest unsubstituted aromatic polyimine

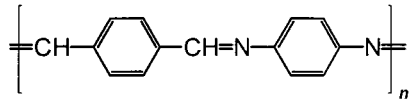

and its dimethoxy derivative

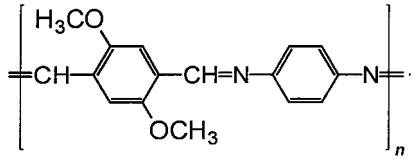

a. Synthesis of Unsubstituted Aromatic Polyimine (PPI)

PPI was prepared from *p*-phenylenediamine and terephthaldehyde using a modification of the method described in (25).

Freshly recrystallized *p*-phenylenediamine (5.4 g) was refluxed with 6.7 g of recrystallized terephthaldehyde in a solution of 10 g of anhydrous sodium acetate in 35 ml of glacial acetic acid. In the course of the reaction a bright yellow polymer precipitated. After 2 h of refluxing the precipitate was separated from the solution; then it was refluxed in 250 ml of dimethylformamide to dissolve unreacted monomer and condensation products of low molecular weight. Finally the polymer was washed with acetone and dried *in vacuo* for 3 h.

b. Synthesis of Dimethoxy-Substituted Polyimine (PMOPI)

PMOPI was prepared from *p*-phenylenediamine and 2,5-dimethoxyterephthaldehyde using a modification of the method described in (26, 27). Since 2,5-dimethoxyterephthaldehyde is not available commercially it was synthesized following the procedure reported in (28).

The reaction was carried out at room temperature in a 1:1 NMP:HMPA solution (110 ml) to which 2.3 g of LiCl was added. To this reaction medium freshly recrystallized diamine (4.1 g) was added followed by 7.5 g of 2,5-dimethoxyformamide. The reaction medium was vigorously stirred for 48 h. The polymer obtained was precipitated in methanol, filtered, and then washed with water and methanol. Finally it was dried under dynamic vacuum.

c. Doping (Protonation) of PPI and PMOPI with Heteropolyacids

The doping (protonation) of the base form of the synthesized polymers was carried out at room temperature,

TABLE 1

Protonation Levels of Prepared Catalysts Determined by Elemental Analysis: C, H, N, Mo, or W

Types of polymer matrix	PMOPI (or PPI) structural unit : HPA molar ratio in the protonating medium	Protonating level determined per polyimine in the structural unit
PPI (repeat unit: $C_{14}H_{10}N_2$)[a]	1 : 2	PPI$(H_3PMo_{12}O_{40})_{0.709}$
PMOPI (repeat unit: $C_{16}H_{14}N_2O_2$)	1 : 0.025	PMOPI$(H_3PMo_{12}O_{40})_{0.018}$
	1 : 0.05	PMOPI$(H_3PMo_{12}O_{40})_{0.036}$
	1 : 0.1	PMOPI$(H_3PMo_{12}O_{40})_{0.068}$
	1 : 0.25	PMOPI$(H_3PMo_{12}O_{40})_{0.198}$
	1 : 1	PMOPI$(H_3PMo_{12}O_{40})_{0.431}$
	1 : 0.025	PMOPI$(H_3PW_{12}O_{40})_{0.012}$
	1 : 0.05	PMOPI$(H_3PW_{12}O_{40})_{0.038}$
	1 : 0.1	PMOPI$(H_3PW_{12}O_{40})_{0.066}$
	1 : 0.25	PMOPI$(H_3PW_{12}O_{40})_{0.173}$
	1 : 1	PMOPI$(H_3PW_{12}O_{40})_{0.399}$

[a] A more detailed characterization of PPI$(HPA)_y$ samples is given in Ref. (7).

typically for 1–1.5 h, in 0.02 M solution of a given heteropolyacid in acetonitrile. The doped polymer was washed repeatedly with pure acetonitrile to remove the unreacted heteropolyacid. The following acids were used in this study: $H_3PMo_{12}O_{40}$ and $H_3PW_{12}O_{40}$. The doping level can be conveniently varied by changing the ratio of polyimine to heteropolyacid.

d. Spectroscopic Studies

FTIR studies of undoped and doped polyimines were performed in transmission geometry using the pressed pellet technique on a Digilab FTS 60 spectrometer.

Raman spectra were obtained on a Bruker RFS 100 RT Raman spectrometer with a 1064-nm excitation line.

X-Ray photoelectron spectra were recorded on a Escalb 210 spectrometer.

e. X-Ray Diffraction Studies

X-ray diffractograms were obtained on a Seifert-FPM XRD 7 diffractometer using Cu$K\alpha$ radiation.

f. TG and DSC Studies

TG and DSC studies were carried out using a Setaram TGDSC 111 apparatus. The heating rate was 10°C/min.

g. BET Specific Surface Area

BET specific surface area measurements were performed by adsorption of nitrogen at the temperature of liquid N_2 on a Carlo Erba Sorpty 1750 apparatus.

h. Catalytic Tests

Kinetic studies of propylene oxidation and isopropanol conversion were undertaken.

Studies of propylene oxidation kinetics were carried out in a differential reactor (29, 30). The substrates, i.e., oxygen and propylene, were used in the molar ratio of 1.2. The substrates were diluted with nitrogen to achieve an initial concentration of propylene equal to 0.020 molar fraction in the stationary state. A constant flow rate of 15.0 dm^3/h was used throughout the entire experiment. The conversion levels ranged from 5 to 15%. The measurements were performed in the temperature range 441–545 K.

The kinetics of isopropanol conversion were measured on two types of catalysts: freshly prepared ones and those previously used for studies of propylene conversion kinetics. The reaction of isopropanol conversion was carried out in an oxygen-free atmosphere (6, 31). The concentration of isopropanol in nitrogen was 1.45 mol%. Conversion levels ranged from 5 to 20%.

Typically 2 g of the catalysts was used for each measurement. Before measurements all catalysts were standarized in the reactor in a flow of the reaction mixture with the same chemical composition as the mixture used in the catalytic test. The standarization was performed at 120°C for 2 h.

A detailed characterization of the samples used can be found in Table 1.

The reaction products were analyzed chromatographically. Based on the results obtained both selectivity and activation energy were calculated for each catalyst used.

RESULTS AND DISCUSSION

First we must specify the system of chemical formula notation we use throughout the paper for both polyimines doped with heteropolyacids. Assuming the repeat units of $C_{14}H_{10}N_2$ and $C_{16}H_{14}N_2O_2$ for PPI and PMOPI, respectively, we express the doping level as the fraction of heteropolyacid (HPA) molecules, y, per repeat unit, i.e., $(C_{14}H_{10}N_2)(HPA)_y$ or in shortened version PPI$(HPA)_y$ and $(C_{16}H_{14}N_2O_2)(HPA)_y$ or in shortened version PMOPI$(HPA)_y$.

Chemical compositions of all samples studied in this research were determined by elemental analysis (C, H, N, Mo, or W). Since heteropolyacids entering the polymer matrix are hydrated a good fit of the analytical data can be obtained only if the hydration process is taken into account. The final formulas should therefore be expressed as $PPI(HPA)_y(H_2O)_z$ and $PMOPI(HPA)_y(H_2O)_z$. For simplicity in the description of the samples studied we neglect hydration.

Interesting information concerning the interactions of the inserted polyheteroanions with the polyimine matrix can be extracted from analysis of FTIR spectra of samples doped to different levels. In this paper we present the spectra of the $POMPI(H_3PW_{12}O_{40})_y$ system (Fig. 1) but for

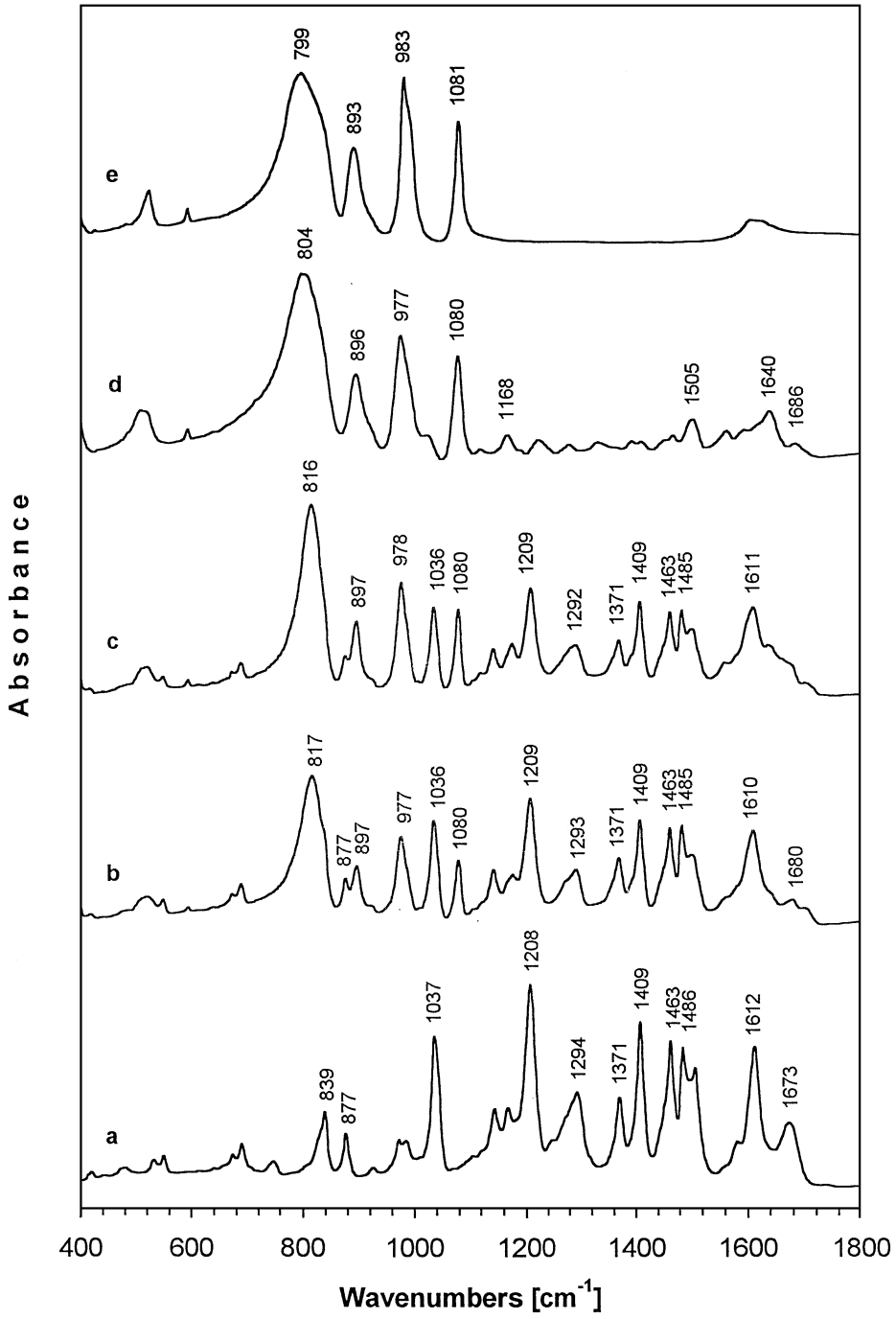

FIG. 1. FTIR spectra of (a) unprotonated PMOPI, (b) $PMOPI(H_3PW_{12}O_{40})_{0.038}$, (c) $PMOPI(H_3PW_{12}O_{40})_{0.066}$, (d) $PMOPI(H_3PW_{12}O_{40})_{0.399}$, and (e) crystalline $H_3PW_{12}O_{40}$.

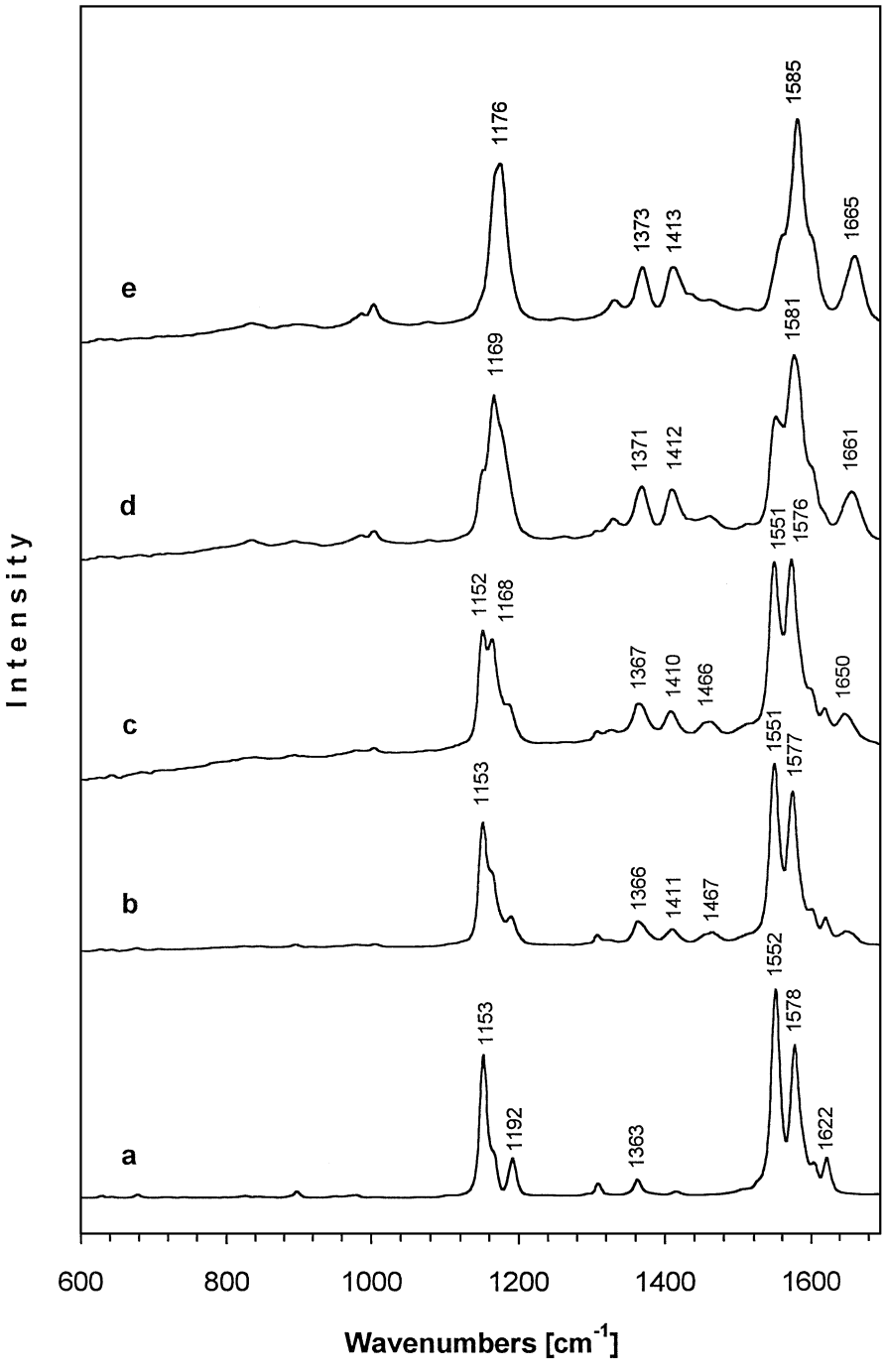

FIG. 2. Raman spectra of (a) unprotonated PPI, (b) PPI$(H_3PW_{12}O_{40})_{0.038}$, (c) PPI$(H_3PW_{12}O_{40})_{0.104}$, (d) PPI$(H_3PW_{12}O_{40})_{0.468}$, and (e) PPI$(H_3PW_{12}O_{40})_{0.804}$.

other aromatic polyimines and other heteropolyacids the doping-induced spectral changes are very similar.

The first and rather obvious conclusion is that the structural identity of the Keggin units characteristic of HPA is preserved on the insertion into the polymer matrix. This is manifested by the presence of four principal bands ascribed to the Keggin structural unit—nM−O_c−M, nM−O_b−M, nM=O_d, nX−O_a (32)—the intensity of which increases with increasing doping level. The position of the band acribed to nM-O_c-M depends on the doping level. For low doping levels it is blue shifted by ca. 25 cm^{-1} with respect to its position in the crystalline heteropolyacid at 799 cm^{-1}. With increasing doping level it approaches the position characteristic of crystalline HPA. We interpret this shift as a measure of the

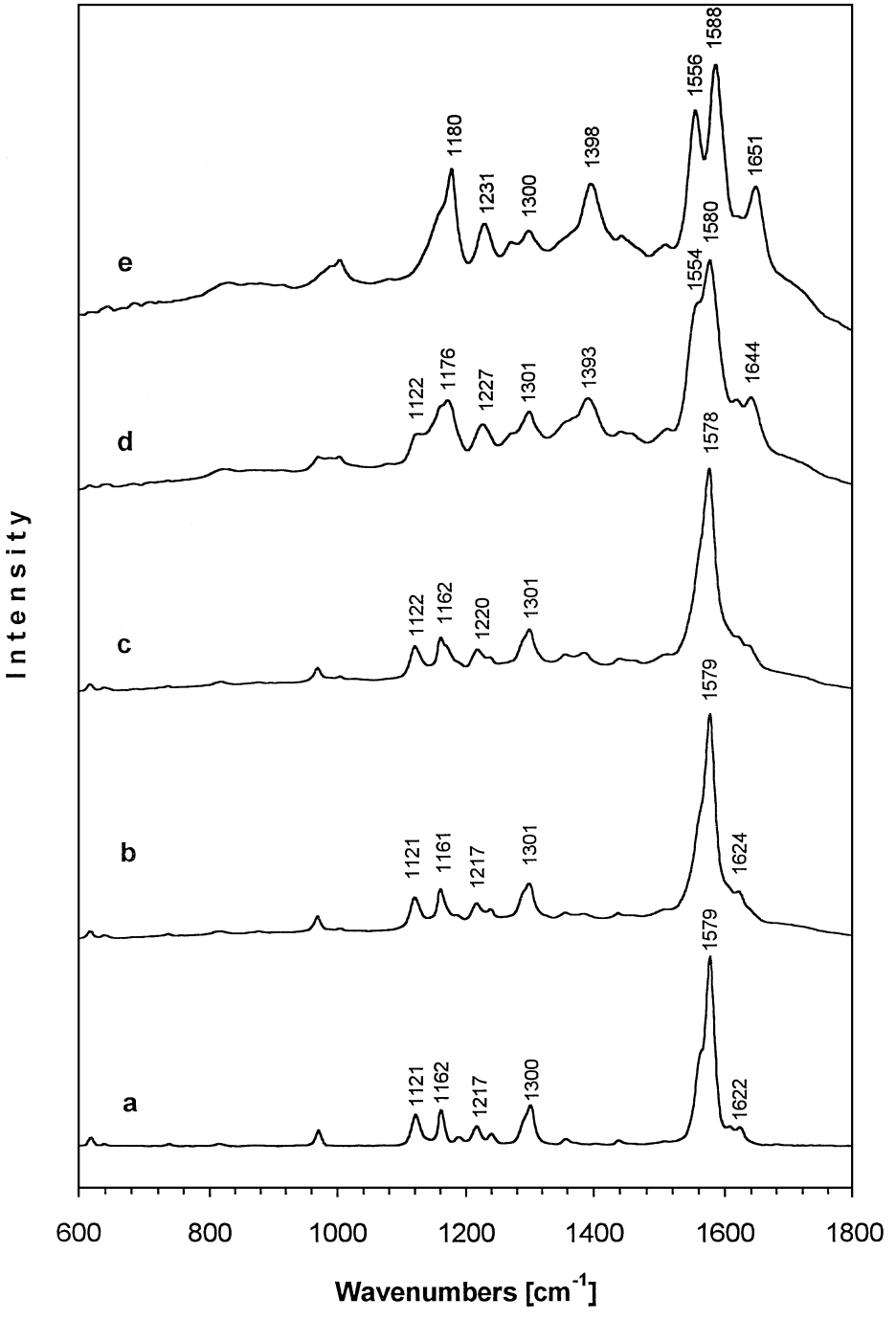

FIG. 3. Raman spectra of (a) unprotonated PMOPI, (b) PMOPI$(H_3PW_{12}O_{40})_{0.038}$, (c) PMOPI$(H_3PW_{12}O_{40})_{0.066}$, (d) PMOPI$(H_3PW_{12}O_{40})_{0.173}$, and (e) PMOPI$(H_3PW_{12}O_{40})_{0.399}$.

interactions between the inserted dopant and the matrix. These interactions occuring via protonation of the imine sites cause some structural deformation of the $[MO_6]$ structural subunit which in turn is manifested by a shift of the nM–O_c–M IR band. Thus at low doping levels the protonation of the matrix by the inserted acid molecules is more efficient. If this interpretation is correct one should expect different selectivity to the products of acid–base catalysis for polyimines doped with HPA to different levels. This is indeed the case (7). In isopropanol conversion PPI$(HPA)_y$ is very selective to acetone for low values of y, whereas for high values of y it acts as a predominantly acid–base catalyst, giving propylene as the main product. Evidently for low y all acid molecules are transformed into the conjugated bases via the protonation reaction with the strongly basic environment of the matrix. As a result all acid–base

centers are blocked and the catalyst acts as a redox catalyst. To the contrary for high values of *y* the majority of acid molecules do not participate in the protonation probably due to steric reasons and can be considered as a source of mobile protons necessary for catalysis of the acid–base type.

Both PPI and PMOPI in their base form give clear Raman spectra (Figs. 2a and 3a). Based on the comparison with low-molecular-weight model compounds (33) and with poly(*p*-phenylene vinylene) (34), which is isoelectronic with PPI, the following attribution of bands is proposed: A weak band at 1622 cm^{-1} observed in both polymers corresponds to the C=N stretching mode. The corresponding band is also observed in the IR spectra; however, in the latter case it is very strong as expected. Two strong bands at 1578 and 1551 cm^{-1} in PPI originate from C=C stretching of the *para*-substituted aromatic bands. In PMOPI the latter band is blue shifted by ca. 10 cm^{-1} and as a result both bands strongly overlap. By analogy with PPV and the model compound the bands at 1363 cm^{-1} in PPI and at 1359 cm^{-1} in PMOPI can be ascribed to C–H deformations in the imine group. Strong bands at 1192 and 1153 cm^{-1} in PPI are attributed to C–C_{ar} stretching and C–H ring deformations, respectively. Contrary to PPI, in PMOPI two bands originating from C–H ring deformations appear at 1162 and 1121 cm^{-1}. This is caused by the presence of two nonequivalent aromatic rings, di- and tetrasubstituted.

The most striking doping-induced Raman spectral change in PPI and PMOPI (Figs. 2 and 3) is strong line broadening caused by amorphization of the sample as evidenced by X-ray diffraction (see below). Due to the protonation reaction that accompanies the doping significant changes are observed in the bands corresponding to the protonation sites (CH=N groupings). The weak band at 1622 cm^{-1} gradually disappears on doping and a new band characteristic of the doped polymer appears at 1665 cm^{-1} in the spectrum of PPI and at 1651 cm^{-1} in the spectrum of PMOPI. The bands due to C=C stretching in the aromatic ring are also influenced. The band at 1578 cm^{-1} in PPI slightly shifts toward higher wavenumbers whereas the band at 1551 cm^{-1} significantly weakens. Two modes observed in IR but inactive in Raman appear at 1467 and 1412 cm^{-1}. These changes indicate that in addition to amorphization of the sample, the doping induces significant conformational changes in the polymer chain.

At the end of the discussion of the Raman data it should be stressed that no lines attributable to heteropolyanions are observed even for high heteropolyanions content. Thus IR and Raman are perfectly complementary in our case; the first technique enables us to follow the deformations in Keggin structural units occuring on insertion into the polymer matrix, whereas the latter method provides evidence of chain conformational changes induced by doping.

Protonation of polyimine basic sites by acidic dopants should also be evidenced by ESCA N 1*s* spectroscopy. Since in basic PPI and PMOPI all nitrogen atoms are spectroscopically equivalent in the N 1*s* spectrum one line is expected with a binding energy characteristic of imine nitrogen. The spectrum of PPI base is shown in Fig. 4a. Indeed the dominant line at 398.7 eV is characteristic of imine nitrogen.

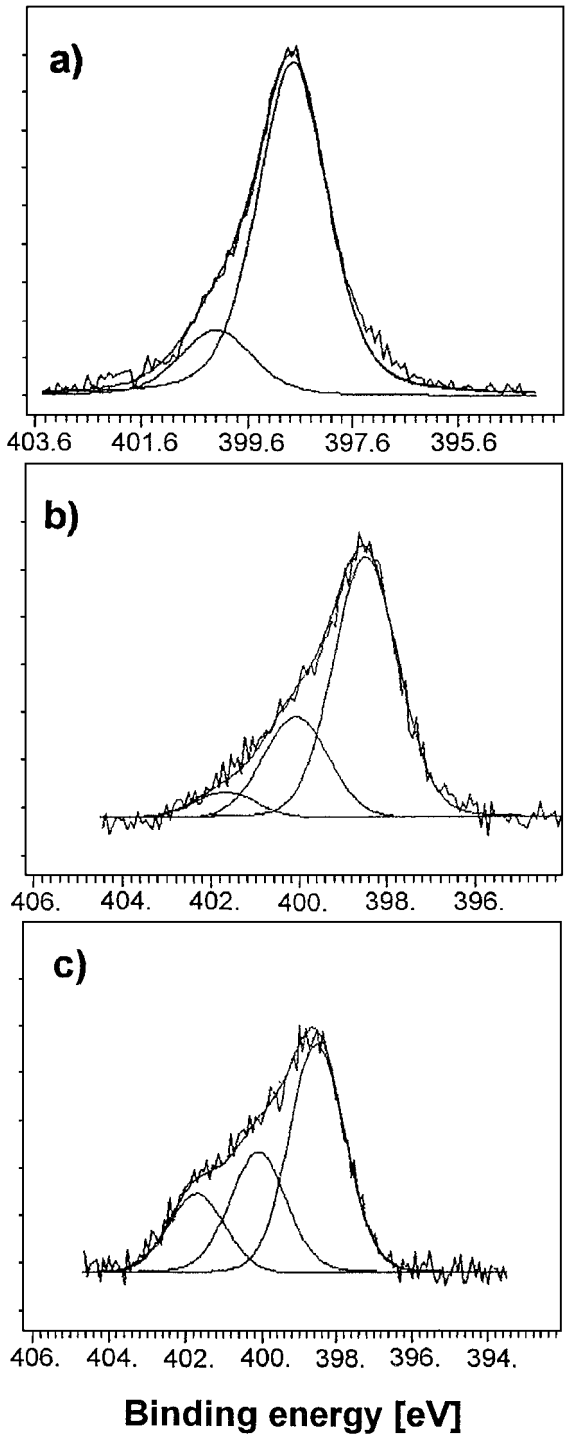

FIG. 4. X-Ray photoelectron N 1*s* spectra of unprotonated PPI (a) and PPI protonated with $H_3PW_{12}O_{40}$: (b) $PPI(H_3PW_{12}O_{40})_{0.104}$, (c) $PPI(H_3PW_{12}O_{40})_{0.804}$.

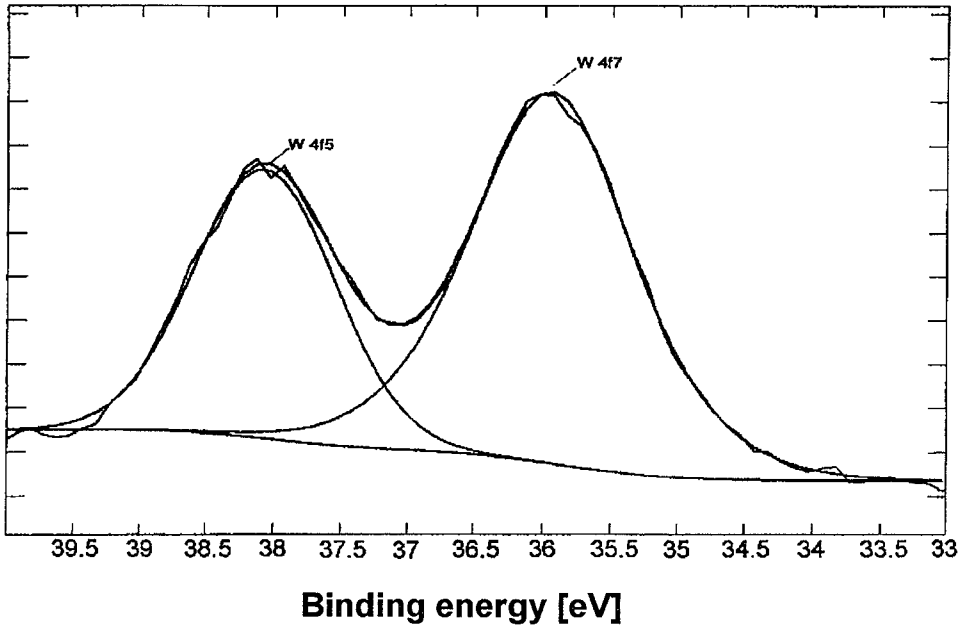

FIG. 5. X-Ray photoelectron W 4*f* spectrum of PPI$(H_3PW_{12}O_{40})_{0.468}$.

However, an additional satellite line of weak intensity is also observed at 400.2 eV. We were unable to get rid of this peak despite careful purification of the sample. Its exact origin is not known at present. The doping with heteropolyacids results in a gradual growth of higher-binding-energy components of the spectrum at the expense of the imine base peak (Figs. 4b and 4c). Such behavior is characteristic of the protonation reaction and has already been observed in polyaniline protonated with heteropolyacids (35). The spectrum can be decomposed into three components at 398.7, 400.2, and 401.8 eV. The last two peaks are in the range characteristic of charged (protonated) nitrogens. This means that in the doped polymer two spectroscopically nonequivalent protonated sites coexist.

In Figs. 5 and 6 W 4*f* and Mo 3*d* are shown for PPI doped with $H_3PW_{12}O_{40}$ and $H_3PMo_{12}O_{40}$, respectively. In the

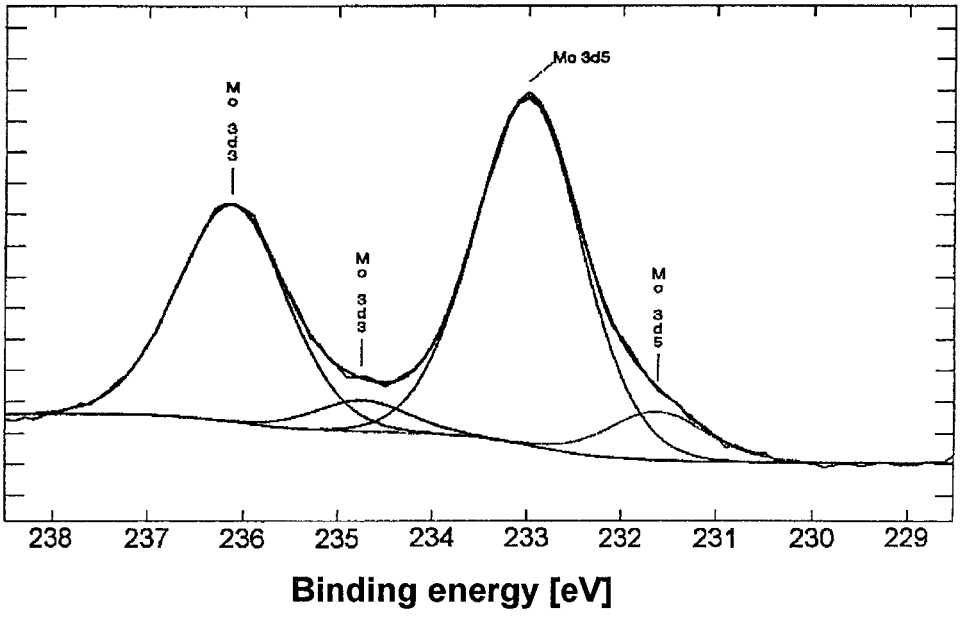

FIG. 6. X-Ray photoelectron Mo 3*d* spectrum of PPI$(H_3PMo_{12}O_{40})_{0.452}$.

spectrum of tungsten only one doublet characteristic of W(VI) is observed which means that the doping with $H_3PW_{12}O_{40}$ is purely acid–base in nature and W does not change its oxidation state on insertion into the polymer matrix. On the contrary, in the case of the doping with $H_3PMo_{12}O_{40}$, the acid–base doping is acompanied by a redox reaction because in the spectrum of Mo 3*d*, in addition to the doublet corresponding to Mo(VI) a weak doublet due to Mo(V) is observed. Thus molybdenum is partially reduced on insertion into PPI.

Doping-induced amorphization of the sample manifested by the broadening of IR and Raman lines can be directly monitored by X-ray diffraction measurements. In Figs. 7 and 8 X-ray diffractograms recorded for increasing doping levels are shown for PPI$(H_3PW_{12}O_{40})_y$ and PMOPI$(H_3PW_{12}O_{40})_y$. Undoped (basic) polymers are surprisingly highly crystalline. The crystallinity index determined using the method of Hindeleh and Johnson is roughly the same for both polyimines, slightly lower than 30%. PMOPI, however, gives broader reflections which means that in this case crystalline domains are smaller. Using the Scherrer formula correlating the size of crystalline domains with the half-width of the Bragg reflections (36),

$$L = \frac{k \cdot \lambda}{B \cdot \cos \Theta},$$

where L = the average size of crystalline domains, B = half-width (in radian units), and k = Scherrer constant (equals about 1). We have calculated the average size of the crystalline zones. In the case of PPI it was 390 Å (based on the reflection peaked at 20.3), whereas for PMOPI it was 215 Å (based on the reflection peaked at 13.9).

On doping the reflections characteristic of the base form gradually disappear, indicating increasing amorphization. No reflections originating from crystalline heteropolyacids can be detected even for the highest doping levels. This means that the doped polymers form a one-phase system in which the dopant molecules are molecularly dispersed. At the highest doping level we observe a new reflection at low Bragg angles which we attribute to one-dimensional ordering of the dopant in the polymer matrix. A similar phenomenon was previously observed for heteropolyacid-doped polyaniline (37).

Spectroscopic and diffraction studies provide significant information concerning the molecular and supramolecular structures of doped polyimines. However, from the catalytic point of view, such properties as the value of specific surface or thermal stability are equally important.

Similarly as in the case of heteropolyacid-doped polyaniline (38), for PPI specific surface area monotonically decreases with the increase in doping level (Fig. 9). Evidently heteropolyacids attached to the surface via the

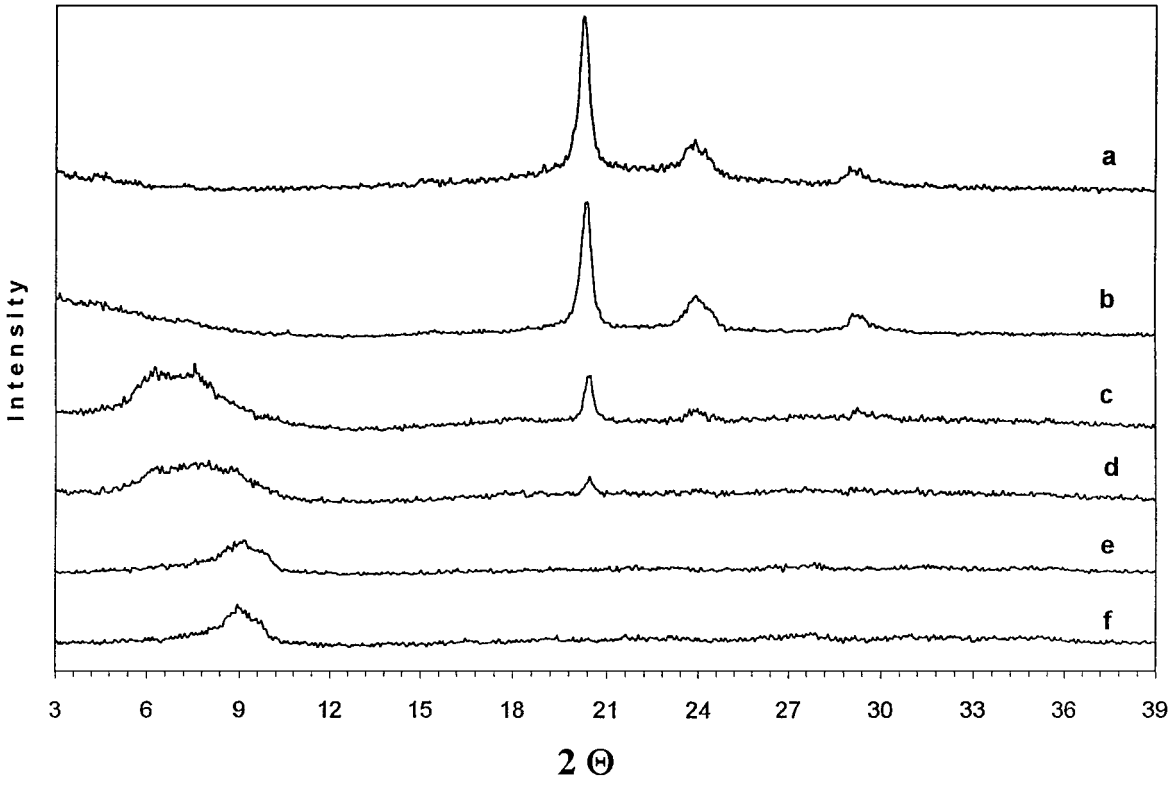

FIG. 7. X-ray diffractograms of (a) unprotonated PPI, (b) PPI$(H_3PW_{12}O_{40})_{0.003}$, (c) PPI$(H_3PW_{12}O_{40})_{0.038}$, (d) PPI$(H_3PW_{12}O_{40})_{0.104}$, (e) PPI$(H_3PW_{12}O_{40})_{0.468}$, and (f) PPI$(H_3PW_{12}O_{40})_{0.804}$.

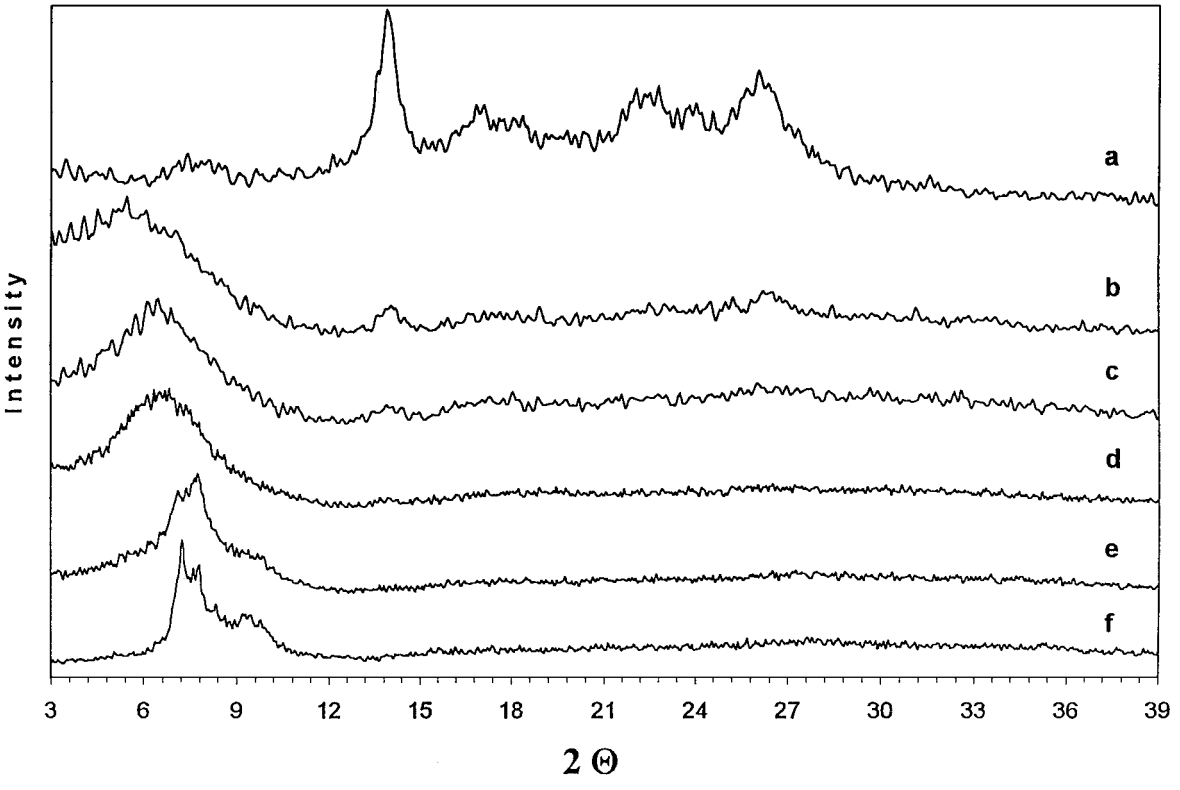

FIG. 8. X-ray diffractograms of (a) unprotonated PMOPI, (b) PMOPI$(H_3PW_{12}O_{40})_{0.012}$, (c) PMOPI$(H_3PW_{12}O_{40})_{0.038}$, (d) PMOPI$(H_3PW_{12}O_{40})_{0.066}$, (e) PMOPI$(H_3PW_{12}O_{40})_{0.173}$, and (f) PMOPI$(H_3PW_{12}O_{40})_{0.399}$.

protonation reaction lower the porosity of the system. The behavior of PMOPI is different. In this case the specific surface area increases with *y* for low doping levels and then begins to decrease (Fig. 10). Probably light doping causes disintegration of agglomerates present in the polymer. When this process is complete further doping leads to a decrease in the remaining porosity.

The thermal stability of $H_3PW_{12}O_{40}$-doped PPI is excellent for a polymeric system. A typical TG, DTG, DSC sets of curves are shown in Figs. 11 and 12. Since heteropolyanions inserted into the polymer matrix are hydrated, the small mass loss around 100–120°C is associated with partial dehydration of the dopant. As expected a weak endotherm is observed in this temperature range in the DSC curve. The intensity of this endotherm increases with increasing doping level. Catalyst degradation starts at ca. 280–300°C and is manifested in the DSC line by a set of strongly overlapping exotherms. However, up to 420–440°C no significant mass loss is recorded in TG.

Similar features are observed for $H_3PW_{12}O_{40}$-doped PMOPI; however, in this case the degradation starts at ca.

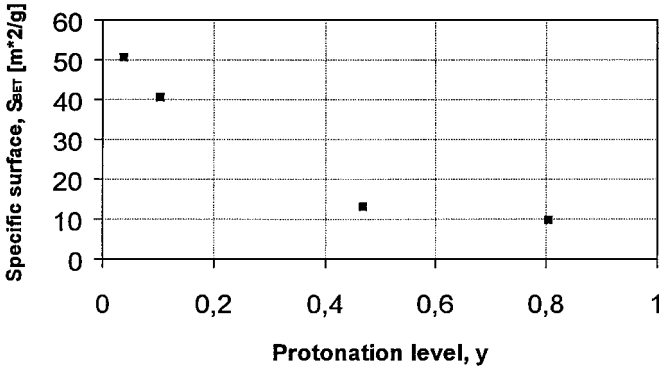

FIG. 9. Specific surface area (S_{BET}) versus protonation level (*y*) of PPI protonated with $H_3PW_{12}O_{40}$.

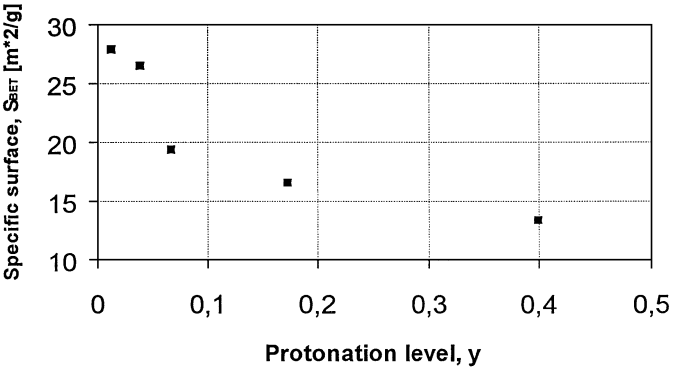

FIG. 10. Specific surface area (S_{BET}) versus protonation level (*y*) of PMOPI protonated with $H_3PW_{12}O_{40}$.

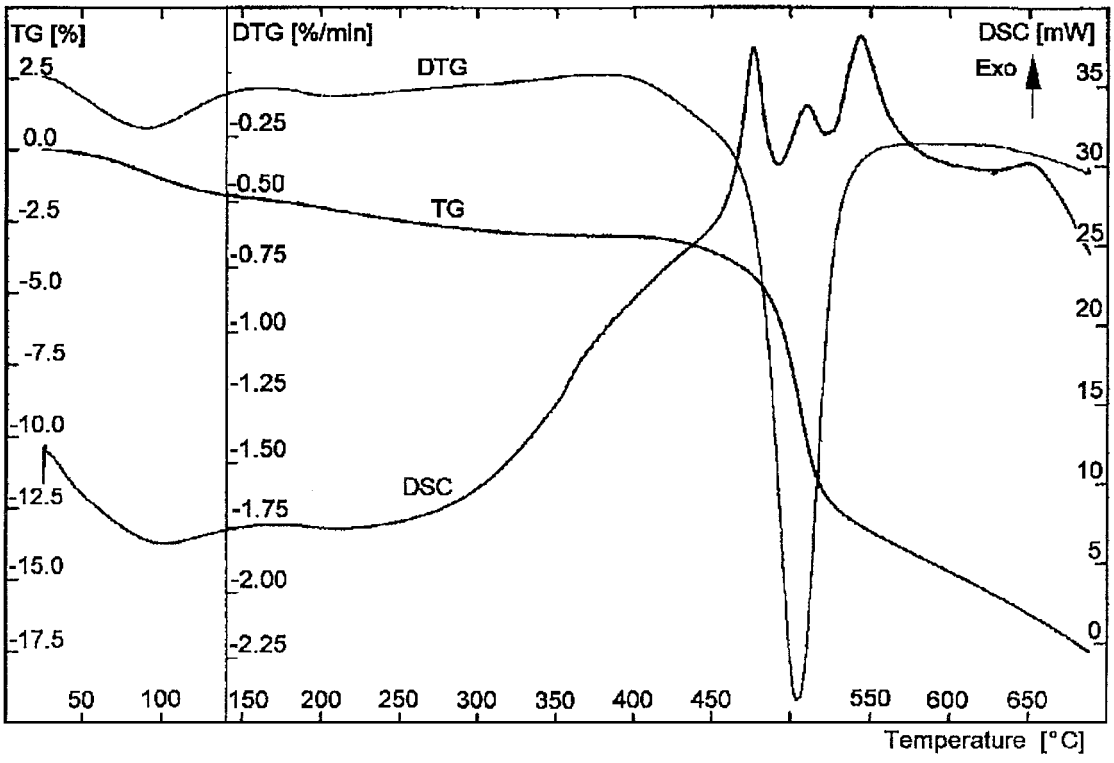

FIG. 11. Thermogravimetric (TG), differential gravimetric (DTG), and differential scanning calorimetry (DSC) set of curves for $PPI(H_3PW_{12}O_{40})_{0.104}$.

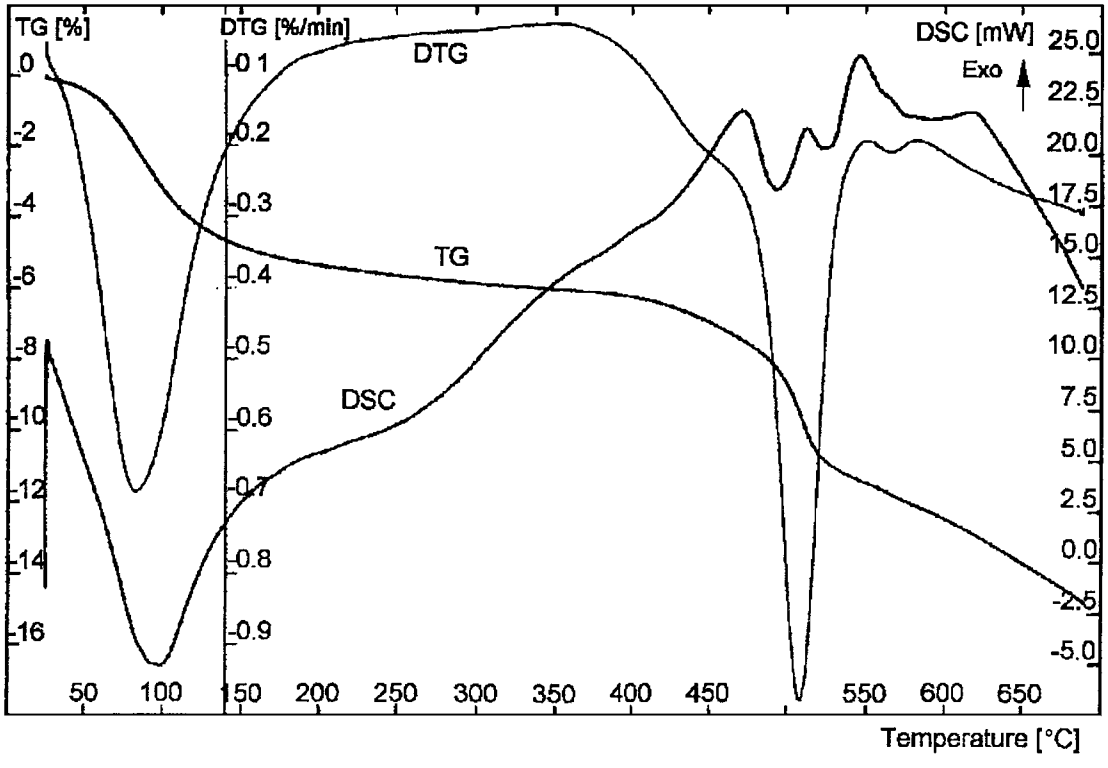

FIG. 12. Thermogravimetric (TG), differential gravimetric (DTG), and differential scanning calorimetry (DSC) set of curves for $PPI(H_3PW_{12}O_{40})_{0.804}$.

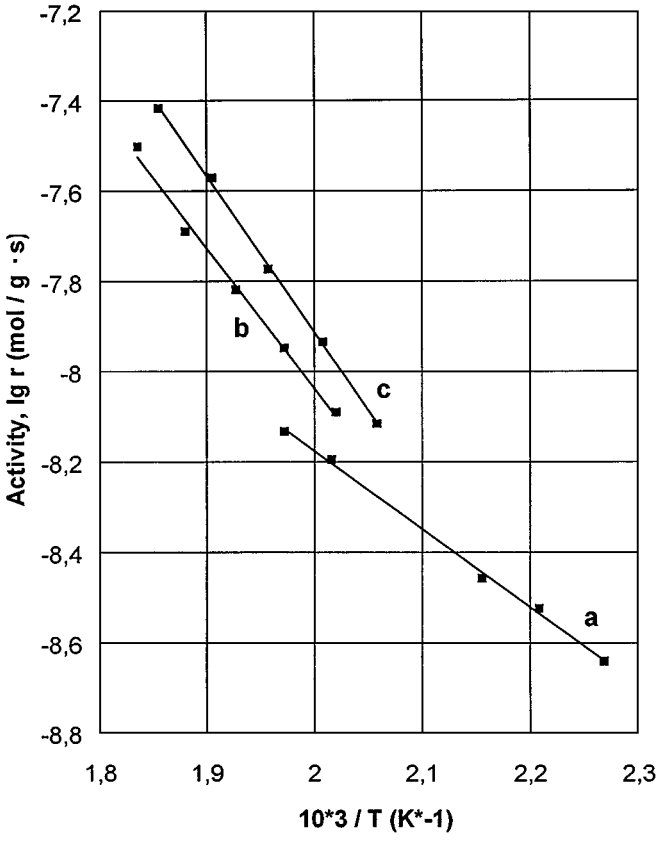

FIG. 13. Arrhenius plots of propylene oxidation over (a) PPI $(H_3PMo_{12}O_{40})_{0.709}$, (b) PMOPI$(H_3PMo_{12}O_{40})_{0.431}$, and (c) PMOPI $(H_3PMo_{12}O_{40})_{0.068}$.

60°C lower temperatures. This also applies to $H_3PM_{12}O_{40}$-doped PPI and PMOPI.

Another question, important from the catalytic point of view, should be addressed, namely, the stability of the catalyst in the presence of the reagents undergoing the catalytic reaction. Since heteropolyacid is chemically bound to the polymer matrix via ionic bonds it cannot be leached out by isopropanol or ethylene or any other reagent tested. The action of these reagents does not deprotonate the polymer; thus heteropolyanions remain fixed to the basic sites of the polymer matrix in the course of the catalytic reaction.

The results of catalytic tests are shown in Figs. 13–16. The kinetic data are presented as the logarithm of the observed reaction rate versus the reciprocal of the absolute reaction temperature. For comparative reasons all data have been normalized to 1 g of heteropolyacid in the catalyst. By this procedure the contribution of catalytically inactive polymer matrix to the mass of the catalyst is eliminated.

The calculated activation energies and selectivities are collected in Tables 2–4. As expected in the reaction of propylene oxidation $H_3PW_{12}O_{40}$ catalysts turned out to be less active than $H_3PMo_{12}O_{40}$ catalysts. Surprisingly, the less active catalysts show much lower activation energy. This may suggest that the reaction takes place in the diffusion limit. However, low reaction temperature seems to exclude this hypothesis.

In principle one can imagine the slowing down of the transport of oxygen by the polymer matrix which would make the diffusion process the limiting step of the reaction. However, if the reaction occurred in the diffusion limit the activation energy would be lower for catalysts containing less heteropolyacid (for low protonation levels the interactions between the matrix and the dopant are stronger and the ratio of matrix molecules to heteropolyacid molecules is higher). The experiment shows the opposite.

In the reaction of isopropanol conversion on freshly prepared polymer-supported $H_3PMo_{12}O_{40}$ catalysts, containing different amounts of heteropolyacid, catalytic activity seems to be independent of heteropolyacid concentration, i.e., the activity normalized per 1 g of heteropolyacid is very similar for all catalysts tested. However, for catalysts used previously for propylene oxidation the measured activity is higher. This increase in activity is especially pronounced in the case of the catalyst containing the largest amount of HPA, i.e., PMOPI$(H_3PW_{12}O_{40})_{0.431}$.

In all cases studied propylene oxidation reaction carried out prior to isopropanol conversion causes an increase in

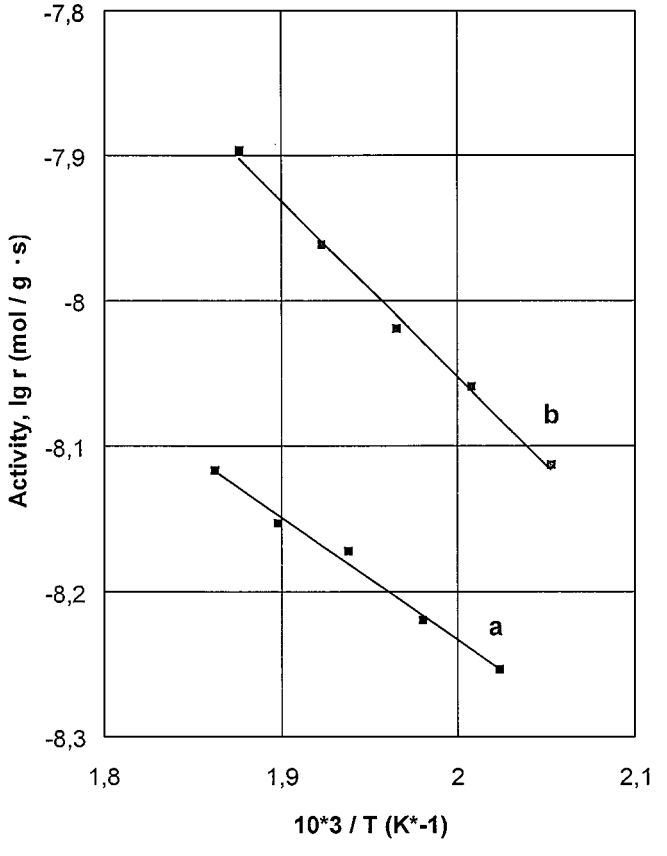

FIG. 14. Arrhenius plots of propylene oxidation over (a) PMOPI$(H_3PW_{12}O_{40})_{0.399}$ and (b) PMOPI$(H_3PW_{12}O_{40})_{0.066}$.

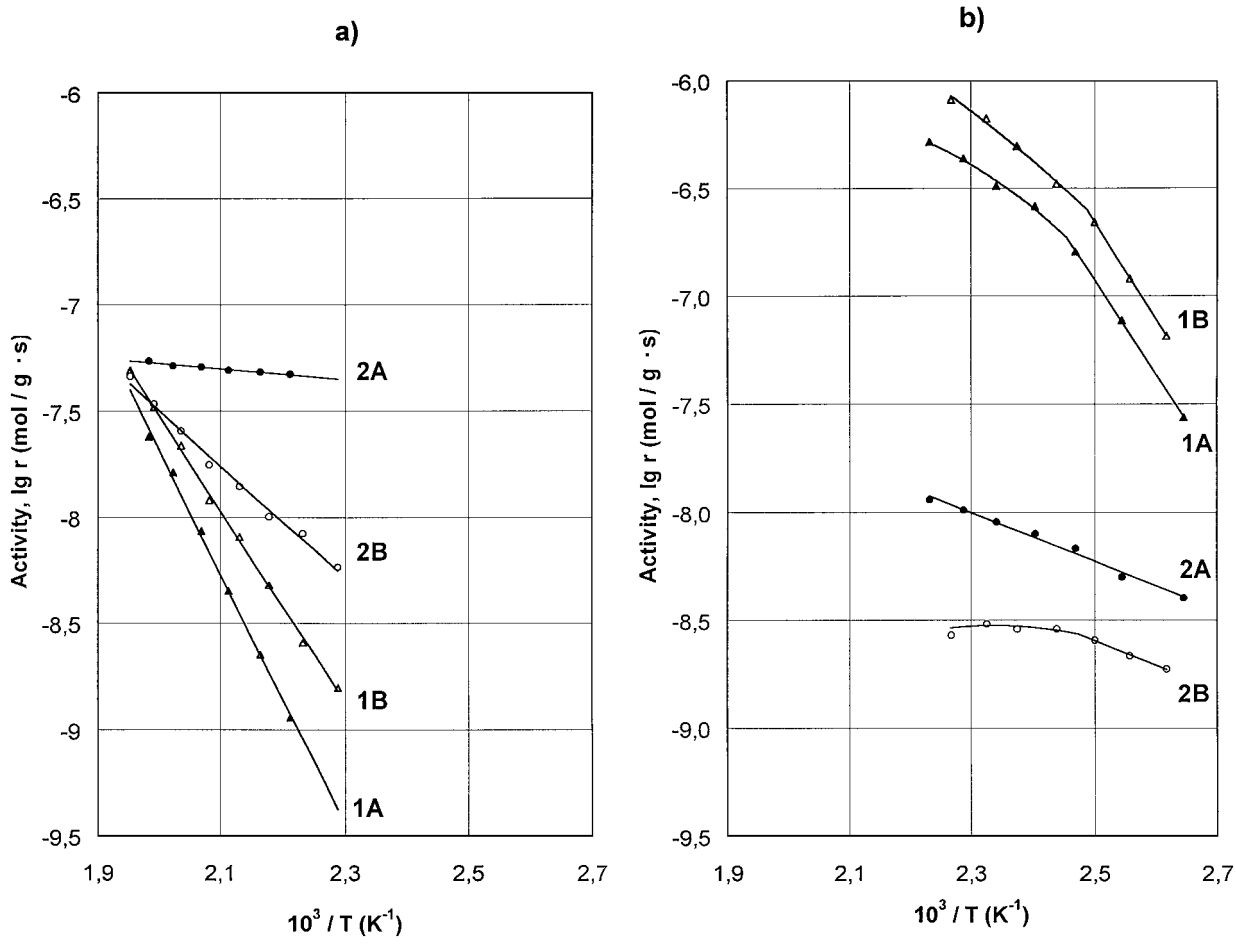

FIG. 15. Arrhenius plots of isopropanol decomposition over catalytic samples: (a) PMOPI$(H_3PW_{12}O_{40})_{0.066}$, (b) PMOPI$(H_3PW_{12}O_{40})_{0.399}$. (1) Propylene; (2) acetone. (A) Freshly prepared catalysts, (B) catalysts used previously for the propylene oxidation reaction.

activity and simultanously a significant decrease in the activation energy of the dehydration reaction. This observation may suggest that some of the protons previously inactive are activated via propylene oxidation process.

Despite the rather high temperature of the process of propylene oxidation (272°C) no thermal destruction of the catalyst takes place. This high thermal stability concerns both the polymer matrix and the heteropolyacid

TABLE 2

Selectivities and Activation Energies of the Catalytic Propylene Oxidation Reaction

Catalyst	HPA content in the sample (wt%)	Temperature (K)	Selectivity (%)					Activation energy (kJ/mol)
			Propionaldehyde	Acetone	Acrolein	Benzene	Hexadiene	
PPI$(H_3PMo_{12}O_{40})_{0.709}$	86.3	464	—	—	2.8	—	97.2	33.7
		496	8.3	—	85.6	—	6.1	
PMOPI$(H_3PMo_{12}O_{40})_{0.431}$	71.8	495	—	4.5	4.9	—	90.6	59.6
		532	0.9	3.9	18.0	—	77.2	
PMOPI$(H_3PMo_{12}O_{40})_{0.068}$	29.8	498	—	1.1	19.9	—	79.0	64.7
		539	2.0	4.4	20.8	—	72.8	
PMOPI$(H_3PW_{12}O_{40})_{0.399}$	72.7	505	—	—	29.3	32.5	38.2	16.2
		527	—	—	25.4	21.1	53.5	
PMOPI$(H_3PW_{12}O_{40})_{0.066}$	38.2	487	—	—	11.7	—	88.3	22.8
		509	—	—	15.8	—	84.2	

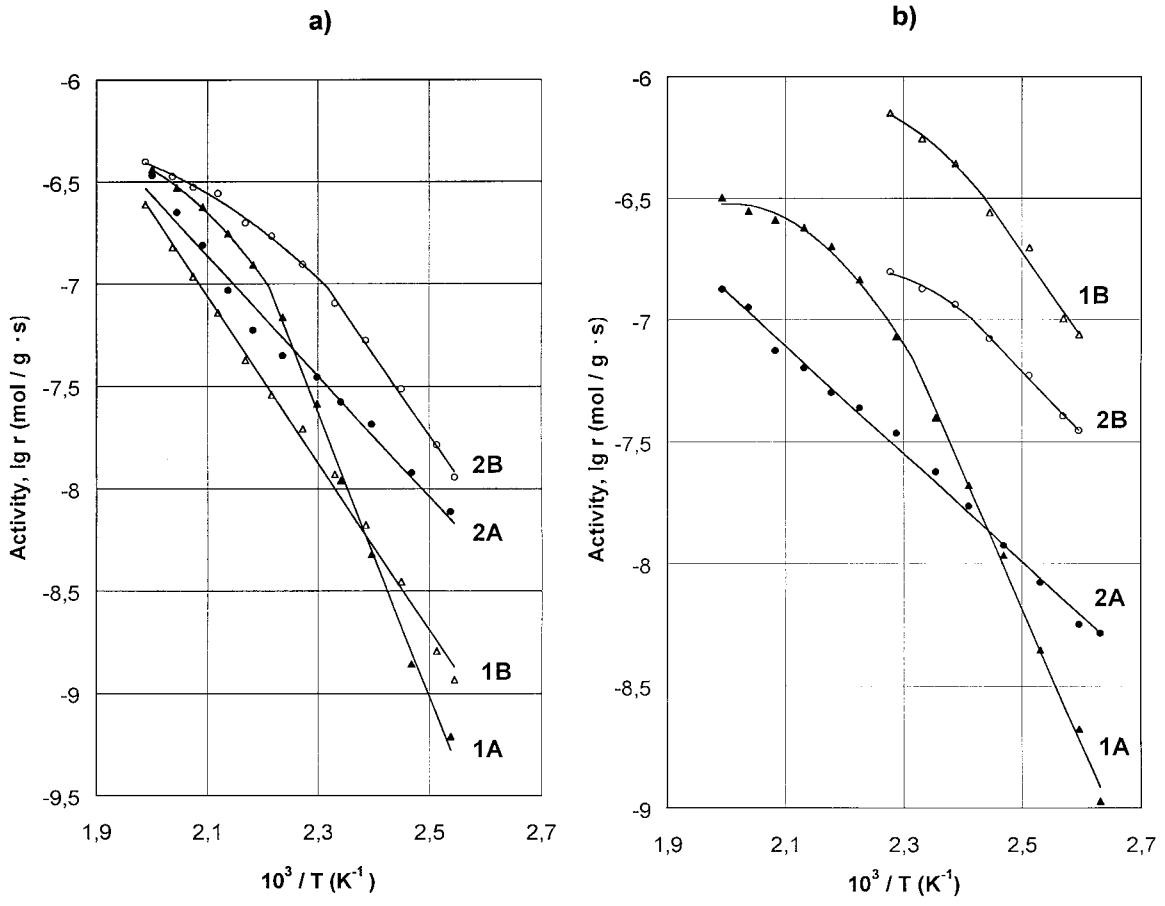

FIG. 16. Arrhenius plots of isopropanol decomposition over catalytic samples: (a) PMOPI($H_3PMo_{12}O_{40}$)$_{0.068}$, (b) PMOPI($H_3PMo_{12}O_{40}$)$_{0.431}$. (1) Propylene, (2) acetone. (A) Freshly prepared catalysts, (B) catalysts used previously for the propylene oxidation reaction.

dopant. Evidently the polymer matrix stabilizes the inserted molecules of heteropolyacids. This conclusion is corroborated by the determination of the catalyst activity in isopropanol conversion. Thermal destruction of heteropolyacids would inevitably lead to a decrease in the number of acidic centers (mobile protons). This in turn would result in a significant decrease in the dehydration reaction rate. The experiment shows the opposite.

TABLE 3

Selectivities of the Catalytic Isopropanol Decomposition Reaction Measured for (a) PMOPI($H_3PMo_{12}O_{40}$)$_y$ Catalysts and (b) PMOPI($H_3PW_{12}O_{40}$)$_y$ Catalysts

Catalyst[a]	HPMo/HPW content of sample (wt%)	Selectivity at 440 K (%)	
		Propylene	Acetone
a. PMOPI($H_3PMo_{12}O_{40}$)$_y$ catalysts			
A PMOPI($H_3PMo_{12}O_{40}$)$_{0.068}$	29.8	43.7	56.3
B PMOPI($H_3PMo_{12}O_{40}$)$_{0.068}$	29.8	11.8	88.2
A PMOPI($H_3PMo_{12}O_{40}$)$_{0.431}$	71.8	75.3	24.7
B PMOPI($H_3PMo_{12}O_{40}$)$_{0.431}$	71.8	81.3	18.6
b. PMOPI($H_3PW_{12}O_{40}$)$_y$ catalysts			
A PMOPI($H_3PW_{12}O_{40}$)$_{0.066}$	38.2	1.1	98.9
B PMOPI($H_3PW_{12}O_{40}$)$_{0.066}$	38.2	23.2	76.8
A PMOPI($H_3PW_{12}O_{40}$)$_{0.399}$	72.7	97.7	2.3
B PMOPI($H_3PW_{12}O_{40}$)$_{0.399}$	72.7	99.6	0.4

[a] (A) Freshly prepared catalysts, (B) catalysts used previously for the propylene oxidation reaction.

TABLE 4

Activation Energies of the Catalytic Isopropanol Decomposition Reaction Measured for (a) PMOPI($H_3PMo_{12}O_{40}$)$_y$ Catalysts and (b) PMOPI($H_3PW_{12}O_{40}$)$_y$ Catalysts

Catalyst[a]	HPMo/HPW content of sample (wt%)	Activation energy (kJ/mol)	
		Dehydration reaction	Dehydrogenation reaction
	a. PMOPI($H_3PMo_{12}O_{40}$)$_y$ catalysts		
A PMOPI($H_3PMo_{12}O_{40}$)$_{0.067}$	29.8	133.3	57.7
B PMOPI($H_3PMo_{12}O_{40}$)$_{0.067}$	29.8	79.7	79.3
A PMOPI($H_3PMo_{12}O_{40}$)$_{0.430}$	71.8	106.3	43.2
B PMOPI($H_3PMo_{12}O_{40}$)$_{0.430}$	71.8	70.2	46.0
	b. PMOPI($H_3PW_{12}O_{40}$)$_y$ catalysts		
A PMOPI($H_3PW_{12}O_{40}$)$_{0.066}$	38.2	113.2	5.4
B PMOPI($H_3PW_{12}O_{40}$)$_{0.066}$	38.2	84.0	51.1
A PMOPI($H_3PW_{12}O_{40}$)$_{0.390}$	72.7	88.4	23.9
B PMOPI($H_3PW_{12}O_{40}$)$_{0.390}$	72.7	83.3	22.2

[a] (A) Freshly prepared catalysts, (B) catalysts used previously for the propylene oxidation reaction.

An increase in the activity of the catalysts used previously for propylene oxidation can be rationalized by the assumption of diffusion of the heteropolyacid molecules from the bulk of the polymer to its surface.

The phenomenon of diffusion of the catalyst active phase toward the catalyst surface, induced by the reagents, has previously been observed for oxide as well as metal alloy catalysts (39). This concept of diffusion is additionally corroborated by the fact that the increase in catalytic activity is more pronounced for catalysts with higher content of the active phase.

For all catalysts studied only products of nondestructive oxidation can be detected. These are acrolein, hexadiene, propionaldehyde, acetone, and benzene.

In the case of $H_3PMo_{12}O_{40}$ catalysts hexadiene is the dominant product at low temperatures. For all catalytic systems studied the selectivity to hexadiene decreases with increasing temperature, whereas the selectivity to acrolein increases. We interpret this phenomenon as the manifestation of faster reoxidation of heteropolyanions at higher temperatures.

Hexadiene is the product of the recombination of two pi-allyl complexes which are formed at the first stage of propylene molecule activation on transition metal ions of the catalyst. The reoxidation of the catalyst must be slow in this case.

The recombination of two allyl complexes accompanied by dehydrogenation results in the formation of benzene. We observe small amounts of this product only in the case of PMOPI($H_3PW_{12}O_{40}$)$_{0.399}$ catalyst.

If during the catalytic process an oxygen atom originating from the Keggin unit is attached and one hydrogen atom is given off, an acrolein molecule is formed. Fast reoxidation of the catalysts favors this process, and as a result under these conditions no hexadiene formation is observed. Also no hexadiene is formed if other than nucleophilic forms of oxygen are present in the system.

If oxygen originating from the Keggin unit is bound to the allyl radical, together with a hydrogen atom detached from the propylene molecule in the process of its activation, propion aldehyde is formed. The selectivity toward this product is, however, very low.

It is interesting to note that for $H_3PMo_{12}O_{40}$ catalysts molecularly dispersed in PMOPI matrix, i.e., the catalysts that produce predominantly hexadiene, high activation energy is measured.

For $H_3PW_{12}O_{40}$ catalysts molecularly dispersed in PMOPI matrix both hexadiene and acrolein are produced.

TABLE 5

Selectivity and Activation Energy of the Catalytic Propylene Oxidation Reaction Measured for $H_3PMo_{12}O_{40}$ on γ-Al_2O_3

Catalyst	HPMo content of sample (wt%)	Temperature (K)	Selectivity (%)			Activation energy (kJ/mol)
			Propionaldehyde	Acrolein	Benzene	
$H_3PMo_{12}O_{40}$ on γ-Al_2O_3	11.7	445	1.7	95.5	2.8	53.6
		475	1.5	97.8	0.7	

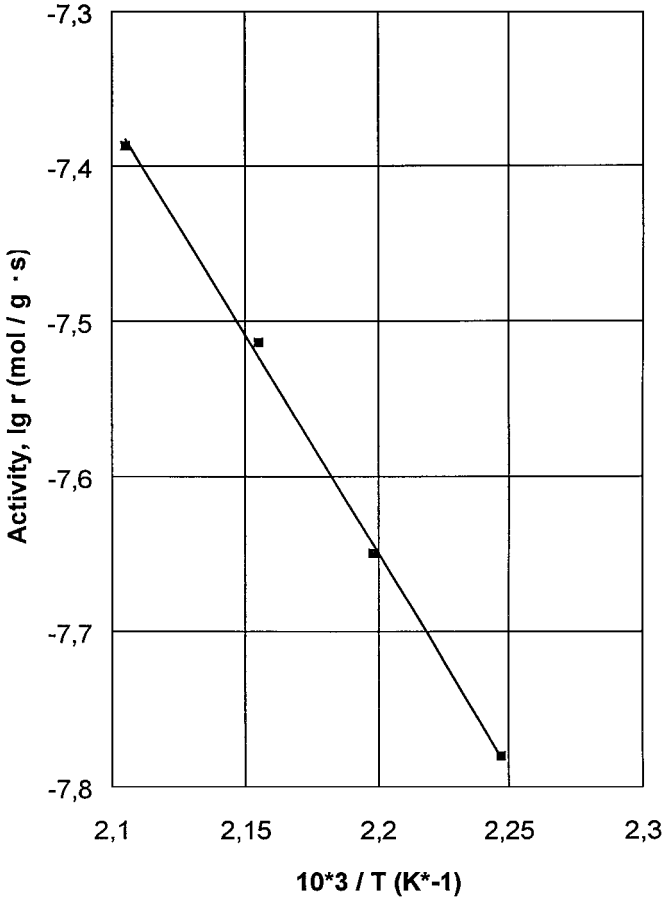

FIG. 17. Arrhenius plots of propylene oxidation over γ-Al_2O_3-supported, crystalline $H_3PMo_{12}O_{40}$.

The ratio of acrolein to hexadiene increases with increasing content of heteropolyacid in the polymer matrix; however, the activation energy of the oxidation reaction decreases.

The prepared catalysts differ significantly from the catalysts obtained by the deposition of $H_3PMo_{12}O_{40}$ on γ-Al_2O_3 which we studied under the same experimental conditions for comparative reasons. In this case acrolein is the dominant product (Table 5, Fig. 17). Interesting catalytic behavior is reported for the PPI$(H_3PMo_{12}O_{40})_y$ sample with high content of heteropolyacid. In this case the activation energy of the oxidation reaction is much lower than for PMOPI$(H_3PMo_{12}O_{40})_y$ catalysts. At low temperatures essentially hexadiene is produced with high selectivity. However, in the case of PPI$(H_3PMo_{12}O_{40})_{0.709}$ an abrupt change in selectivity is observed in the temperature range 191 to 223°C: acrolein is formed instead of hexadiene. This means that the polymer catalyst begins to behave similarly to classic heteropolyacid catalysts.

The lack of electrophilic forms of oxygen in the process of propylene oxydation is not a sufficient condition for the formation of hexadiene. Several steric conditions must also be fulfilled; i.e., the matrix may or may not impose appropriate orientation of the propylene molecule in the course of catalytic reaction. This fact is strongly manifested by the influence of the polymer matrix on the selectivity of the oxidation reaction. For $H_3PMo_{12}O_{40}$ catalysts dispersed in PMOPI no significant decrease in the selectivity to hexadiene is observed with increasing temperature. This is true even for low contents of $H_3PMo_{12}O_{40}$.

CONCLUSIONS

To summarize, we have prepared a new type of polymer-supported catalysts by acid–base-type doping of solid aromatic poly(azomethines) with heteropolyacids. These new catalysts are active in propylene oxidation, exhibiting total selectivity to the products of nondestructive oxidation, with hexadiene as the dominant product. In the case of oxidation to hexadiene two factors play an important role: the lack of electrophilic forms of oxygen and steric effects influenced by the polymer matrix.

The general conclusion derived from this research can be formulated as follows: Since in all polymer-supported catalysts only the products of nondestructive oxidation are detected the formation of products of destructive oxidation (including total combustion) is inherently associated with the presence of electrophilic forms of oxygen which are absent in our systems.

ACKNOWLEDGMENT

This work was financially supported by the Polish Commitee for Scientific Research (KBN) Grant 10.10.160.427.

REFERENCES

1. Nalwa, H. S. (Ed.), "Handbook of Organic Conductive Molecules and Polymers." Wiley, New York, 1997.
2. Skotheim, T. A., Elsenbaumer, R. L., and Reynolds, J. R. (Eds.), "Handbook of Conducting Polymers." Marcel Dekker, New York, 1998.
3. Bidan, G., Genies, E. M., and Łapkowski, M., *J. Electroanal. Chem.* **251**, 297 (1988).
4. Keita, B., Bouaziz, D., and Nadjo, L., *J. Electroanal. Chem.* **255**, 303 (1988).
5. Poźniczek, J., Kulszewicz-Bajer, I., Zagórska, M., Kruczała, K., Dyrek, K., Bielański, A., and Proń, A., *J. Catal.* **132**, 311 (1991).
6. Hasik, M., Turek, W., Stochmal, E., Łapkowski, M., and Proń, A., *J. Catal.* **147**, 544 (1994).
7. Stochmal-Pomarzańska, E., Hasik, M., Turek, W., and Proń, A., *J. Mol. Catal.* **114**, 267 (1996).
8. Haber, J., and Grzybowska, B., *J. Catal.* **28**, 489 (1973).
9. Linde, W. R., Margolis, L. J., and Rogiński, S. Z., *Dokl. Akad. Nauk SSSR* **136**, 360 (1961).
10. Kurina, L. N., Kowal, L. M., and Kotienko, N. F., *Z. Fiz. Chim.* **49**, 1494 (1975).
11. Kowal, L. M., and Kurina, L. N., *Z. Fiz. Chim.* **51**, 889 (1977).
12. Ansic, A. G., Sokolowskij, W. S., and Boreskow, G. K., *Kinet. Katal.* **15**, 1033 (1974).
13. Matsuura, Y., and Schmit, G. C. A., *J. Catal.* **20**, 19 (1971).
14. Haber, J., Mielczarska, E., and Turek, W., *React. Kinet. Catal. Lett.* **34**, 45 (1987).

15. Turek, W., *Przem. Chem.* **69**, 398 (1990).
16. Turek, W., and Suchoń, S., *Pol. J. Appl. Chem.* **36**, 225 (1992).
17. Bielański, A., Haber, J., in "Oxygen in Catalysis." Marcel Dekker, New York, 1991.
18. Haber, J., *Stud. Surf. Sci. Catal.* **72**, 279 (1992).
19. Haber, J., *in* "Proceedings, 8th International Congress on Catalysis, Berlin, 1984," Vol. 1, p. 85. Dechema, Frankfurt-am-Main, 1984.
20. Haber, J., *in* "The Role of Solid State Chemistry in Catalysis" (R. K. Grasselli and J. F. Brazdil, Eds.), ACS Symp. Ser. No. 279, p. 3. Am. Chem. Soc., Washington, DC, 1985.
21. Haber, J., *in* "Heterogenous Catalytic Oxidation" (B. K. Warren and S. Oyama, Eds.), ACS Symp. Ser. No. 638, p. 20. Am. Chem. Soc., Washington, DC, 1996.
22. Missono, M., *Catal. Rev.* **29**, 269 (1987).
23. Missono, M., *in* "Proceedings, 10th International Congress on Catalysis, Budapest, 1992" (M. J. Phillips and M. Ternan, Eds.). Akadémiai Kiadó, Budapest, 1993.
24. Brückman, K., and Haber, J., *in* "Advances in Catalyst Design" (M. Graziani and C. N. R. Rao, Eds.), Vol. 2, p. 111. World Scientific, Singapore, 1993.
25. Manassen, J., and Khalif, S., *J. Am. Chem. Soc.* **88**, 1943 (1966).
26. Morgan, P. W., Kwolek, S. L., and Plechter, T. C., *Macromolecules* **20**, 729 (1987).
27. Yang, C. J., and Jenekhe, S. A., *Chem. Mater.* **3**, 878 (1991).
28. Wood, J. H., and Gibson, E., *J. Am. Chem. Soc.* **71**, 393 (1949).
29. Schwab, G. M., *Chem. Ing. Technol.* **39**, 1191 (1967).
30. Brückman, K., Haber, J., and Turek, W., *J. Catal.* **114**, 196 (1988).
31. Turek, W., Łapkowski, M., and Bidan, G., *Mater. Sci. Forum* **122**, 65 (1993).
32. Rocchiccioli-Deltcheff, C., Thouvenot, F., and Franck, R., *Spectrochim. Acta. A* **32**, 587 (1976).
33. Stochmal-Pomarzańska, E., Ph.D. thesis, University of Mining and Metallurgy. (AGH), Krakow, unpublished.
34. Buisson, J. P., Lefrant, S., and Louran, G., *Synth. Met.* **49–50**, 305 (1992).
35. Hasik, M., Proń, A., Poźniczek, J., Bielański, A., Piwowarska, Z., Kruczała, K., and Dziembaj, R., *J. Chem. Soc. Faraday Trans.* **90**, 2099 (1994).
36. Rabiej, S., *Eur. Polym. J.* **27**, 947 (1991).
37. Łużny, W., and Hasik, M., *Solid State Commun.* **99**, 685 (1996).
38. Hasik, M., Proń, A., Raynor, J. B., and Łużny, W., *New J. Chem.* **19**, 1155 (1995).
39. Haber, J., Mielczarska, E., and Turek, W., *Z. Phys. Chem.* **144**, 69 (1985).